Molecular and Cellular Endocrinology 248 (2006) 172–181

Molecular and Cellular Endocrinology

www.elsevier.com/locate/mce

A generalized numerical approach to rapid-equilibrium enzyme kinetics: Application to 17β-HSD

Petr Kuzmič

BioKin Ltd., 1652 South Grand Avenue, Suite 337, Pullman, WA 99163, USA

Abstract

A generalized numerical treatment of rapid-equilibrium enzyme kinetics is presented. This new approach relies on automatic computer derivation of the underlying mathematical model (a system of simultaneous nonlinear algebraic equations) from a symbolic representation of the reaction mechanism (a system of biochemical equations) provided by the researcher. The method allows experimental biochemists to analyze initial-rate enzyme kinetic data without having to use any mathematical equations. An illustrative example is based on the inhibition kinetics of 17β-hydroxysteroid dehydrogenase type 5 by a class of natural compounds. A computer implementation of the new method, a newly modified software package DYNAFIT [Kuzmič, P., 1996. Program DYNAFIT for the analysis of enzyme kinetic data: application to HIV proteinase. Anal. Biochem. 237, 260–273], is freely available to all academic researchers.

Keywords: Enzyme kinetics; Theory; Mathematics; Statistics; Mechanism; Data analysis; Steady state; Multiple simultaneous equilibria; DYNAFIT

1. Introduction

The task of mechanistic enzyme kinetics is to compare available experimental data with the predictions of kinetic theory, and make conclusions about the plausibility of the underlying mechanistic model. Often the experimental data are *initial reaction rates* of an enzyme catalyzed process, in dependence on the total concentrations of reactants. The theoretical model traditionally is an algebraic rate equation, based either on the rapid-equilibrium approximation (Segel, 1975, Chapters 2–8) or on the steady-state approximation (Segel, 1975, Chapter 9).

This paper utilizes a generalized approach to rapid-equilibrium enzyme kinetics, which simultaneously solves two problems. First, the classical enzyme kinetic formalism is restricted to experimental conditions, under which the concentration of the enzyme catalyst is negligibly small. In our generalized approach, this restriction is removed. This generalization creates the possibility of investigating many practically important systems, for which the classical theory is not applicable. For example, when two "tight-binding" inhibitors (Williams and Morrison, 1979) are present simultaneously, a classical rate equation cannot be derived at all (Kuzmič et al., 1992).

The second difficulty with traditional enzyme kinetics is that, even in those cases where a classical rate equation does exist, it is often extremely complicated. For example, the "random Bi–Bi" steady-state mechanism of bisubstrate enzymes leads to a rational polynomial rate equation containing 48 terms in the denominator (Segel, 1975, p. 469). Rapid-equilibrium mechanisms lead to somewhat simple algebraic rate equations, but their complexity can still be daunting to a nonspecialist.

In our approach, no algebraic manipulations are involved at all. The mathematical model for an arbitrarily complex mechanism is represented simply by two matrices, namely, the *formula matrix* (Smith and Missen, 1982) and a newly introduced *stability matrix*. The formula matrix expresses the composition of complex molecular species in terms of components. The stability matrix describes the total stability constants of molecular complexes, in terms of binary dissociation constants.

As an illustrative example, we shall consider a reaction mechanism proposed by Krazeisen et al. (2001) for the inhibition of 17β-hydroxysteroid dehydrogenase type 5 by phytoestrogens. It has been hypothesized that the phytoestrogen inhibitors bind only to the cofactor site on the enzyme, but not to the substrate site. We present a heuristic *simulation study* of

E-mail address: pksci01@biokin.com.
URL: http://www.biokin.com.

0303-7207/$ – see front matter © 2005 Elsevier Ireland Ltd. All rights reserved.
doi:10.1016/j.mce.2005.10.012

a suitable experimental design, which could be used to prove or disprove the proposed structural-binding mode.

2. Methods

This section summarizes mathematical concepts that were used to formulate our generalized numerical approach to rapid-equilibrium enzyme kinetics.

2.1. Theory

We assume that the enzymatic reaction mechanism consists of n_R rapid-equilibrium steps, in which the ligands (substrates, inhibitors or activators) reversibly bind to the enzyme. Each ligand-binding step is characterized by the corresponding dissociation constant K_i ($i = 1, 2, \ldots, n_R$). In addition, the reaction mechanism contains a single slow step (either reversible or effectively irreversible), in which bond breaking or bond making occurs. These are the usual assumptions of classical rapid-equilibrium enzyme kinetics (Segel, 1975, Chapters 2–8). However, unlike in the classical treatment, we do not assume that the enzyme catalyst is present in a negligibly small amount.

We shall further assume that all molecular species participating in the reaction mechanism can be categorized into n_E molecular *components* (elements) and n_C molecular *complexes*. The total number of molecular species is $n_S = n_E + n_C$. The composition of molecular complexes is described by the *formula matrix* **F** (Smith and Missen, 1982). The formula matrix has n_E rows and n_S columns. The first n_E columns represent a unit matrix. Matrix elements in the subsequent n_C columns contain positive whole numbers, corresponding to the composition of each molecular complex in terms of components.

The total stability constants (Beck and Nagypál, 1990, p. 12) of each molecular complex are expressed in terms of the binary dissociation constants, in the form of the *stability matrix* **B**. Thus, the stability matrix relates to the presumed reaction mechanism. The matrix has n_R rows and n_S columns. The first n_E columns, corresponding to the component species, are filled with zeros. Matrix elements in the subsequent n_C columns are either zero or minus one, depending on the reaction mechanism. An illustrative example is given in Section 3 below.

2.1.1. Mass-conservation law

According to the mass-action law, the concentration of each species at equilibrium is given by Eq. (1), where β_j is the is the total stability constant for the formation of the jth molecular complex from component species. The stability constant is defined in terms of the constants according to Eq. (2), where $B_{i,j}$ are elements of the stability matrix. The mass-conservation law for component species is expressed in the system of n_E simultaneous nonlinear algebraic Eq. (3) for n_E unknowns (c_i, $i = 1, 2, \ldots, n_E$), where the "tilde" accent $\tilde{c}$ represents the total or analytic concentration of component species.

$$c_j = \beta_j \prod_{i=1}^{n_E} c_i^{F_{i,j}}; \qquad j = 1, 2, \ldots, n_S \tag{1}$$

$$\beta_j = \prod_{j=1}^{n_R} K_i^{B_{i,j}}; \qquad j = 1, 2, \ldots, n_S \tag{2}$$

$$\sum_{j=1}^{n_S} F_{i,j} c_j - \sum_{j=1}^{n_S} F_{i,j} \tilde{c}_j = 0; \qquad i = 1, 2, \ldots, n_E \tag{3}$$

2.1.2. Multidimensional Newton–Raphson method

The theory of the iterative Newton–Raphson method in multiple dimensions is described in detail elsewhere (Press et al., 1992, pp. 379–383). When this general theory is applied to rapid-equilibrium enzyme kinetics, we solve a system of n_E nonlinear algebraic Eq. (3) for the concentrations of component species at equilibrium.

We begin with an initial estimate of the solution vector, and then refine this estimate in a series of iterations according to Eq. (4), where α is a heuristic parameter (usually $\alpha = 1$). In the mth iteration, the correction vector $\delta\mathbf{c}^{(m)}$ is found by solving a $n_E \times n_E$ linear algebraic system (5), where **J** is the Jacobian matrix of derivatives defined by Eq. (7). The iterations are repeated until the correction vector $\delta\mathbf{c}$ becomes sufficiently small (see below).

$$\mathbf{c}^{(m+1)} = \mathbf{c}^{(m)} + \alpha \times \delta\mathbf{c}^{(m)} \tag{4}$$

$$\mathbf{J}^{(m)} \cdot \delta\mathbf{c}^{(m)} = \mathbf{f}^{(m)} \tag{5}$$

$$f_i^{(m)} = \sum_{j=1}^{n_S} F_{i,j} c_j^{(m)} - \sum_{j=1}^{n_S} F_{i,j} \tilde{c}_j; \qquad i = 1, 2, \ldots, n_E \tag{6}$$

$$J_{i,j}^{(m)} = \sum_{k=1}^{n_S} F_{j,k} F_{i,k} \frac{c_k^{(m)}}{c_j^{(m)}}; \qquad i, j = 1, 2, \ldots, n_E \tag{7}$$

2.1.3. First derivatives of equilibrium concentrations

The equilibrium composition of complex biochemical mixtures depends on two types of state parameters, namely, the dissociation constants K_i ($i = 1, \ldots, n_R$) and the total concentrations of components species $\tilde{c}_i$ ($i = 1, \ldots, n_E$). The first derivatives of component concentrations with respect to the given state parameter p are obtained by solving the system of simultaneous linear Eq. (8).

$$\begin{pmatrix} J_{1,1} & \cdots & J_{1,n_E} \\ \vdots & \ddots & \vdots \\ J_{n_E,1} & \cdots & J_{n_E,n_E} \end{pmatrix} \begin{pmatrix} \frac{\partial c_1}{\partial p} \\ \vdots \\ \frac{\partial c_{n_E}}{\partial p} \end{pmatrix} = - \begin{pmatrix} \frac{\partial f_1}{\partial p} \\ \vdots \\ \frac{\partial f_{n_E}}{\partial p} \end{pmatrix} \tag{8}$$

The first derivatives of complex concentrations are obtained as is shown in Eq. (9). (In the notation $i = n_E + 1, \ldots, n_S$ it is assumed that the species are ordered in such a way that the components are followed by the complexes.) The final formulas (10)–(13) are derived in Appendix A.1.

$$\frac{\partial c_j}{\partial p} = \frac{\partial}{\partial p} \left\{ \beta_j \prod_{i=1}^{n_E} c_i^{F_{i,j}} \right\}; \qquad j = n_E + 1, \ldots, n_S \tag{9}$$

$$\frac{\partial f_i}{\partial K_u} = \sum_{j=1}^{n_S} F_{i,j} \frac{B_{u,j} c_j}{K_u}; \qquad i = 1, \cdots, n_E \tag{10}$$

$$\frac{\partial c_j}{\partial K_u} = c_j \left(\sum_{i=1}^{n_E} F_{i,j} \frac{\partial \ln c_i}{\partial K_u} + \frac{B_{u,j}}{K_u} \right); \qquad j = n_E + 1, \cdots, n_S \tag{11}$$

$$\frac{\partial f_i}{\partial \tilde{c}_u} = - \sum_{j=1}^{n_S} F_{i,j} \delta_{u,j}; \qquad i = 1, \cdots, n_E \tag{12}$$

$$\frac{\partial c_j}{\partial \tilde{c}_u} = c_j \sum_{i=1}^{n_E} F_{i,j} \frac{\partial \ln c_i}{\partial \tilde{c}_u}; \qquad j = n_E + 1, \cdots, n_S \tag{13}$$

2.2. Implementation

A practical implementation of the theoretical principles described above involves (i) making the initial estimate of equilibrium concentrations, (ii) checking the physical meaning of intermediate results, (iii) utilizing a suitable convergence criterion and (iv) a convenient way of solving the linear system (5) to facilitate the computation of derivatives. The computational algorithm is controlled by three empirical parameters, γ_1–γ_3, which are defined below.

2.2.1. Initial estimate

In a closely related *unidimensional* iterative method we have described previously (Kuzmič, 1998), the initial estimate of component concentrations is set to the corresponding total or analytic concentrations, while the initial estimate of complex concentrations is set to zero. Such choice is not practical in the *multidimensional* Newton–Raphson method, because some elements of the Jacobian matrix (7) could not be evaluated (division by zero). Thus, according to Eq. (14), initial estimates of equilibrium concentrations are always positive numbers. If the analytic concentration of a species (either a component or a complex) is nonzero, that value is also used as the initial estimate of the equilibrium concentration. On the other hand, if the analytic concentration of a species is zero, a small fraction of the smallest analytic concentration is used. A suitable value of the empirical parameter is $\gamma_1 = 0.0001$.

$$c_i^{(0)} = \begin{cases} \tilde{c}_i, & \text{if } \tilde{c}_i \neq 0 \\ \gamma_1 \min(c_1, c_2, \ldots, c_{n_S}), & \text{if } \tilde{c}_i = 0 \end{cases} ; \quad i = 1, \cdots, n_S \tag{14}$$

2.2.2. Positivity of the solution

In each iteration, the corrections, $\delta\mathbf{c}^{(m)}$ in Eq. (5), are checked for physical meaning. In particular, it must be ensured that all component concentrations remain positive. If the proposed correction is too large and negative, the component concentration is set to a certain fraction of the current estimate. Thus, the $(m+1)$th estimate of the equilibrium concentrations is made according to Eq. (15). A suitable value of the empirical parameter is $\gamma_2 = 0.1$.

$$\alpha = \begin{cases} 1 & \text{if } \delta c_i^{(m)} < c_i^{(m)} \\ \gamma_2 c_i^{(m)} & \text{if } \delta c_i^{(m)} \geq c_i^{(m)} \end{cases} ; \qquad i = 1, \cdots, n_E \tag{15}$$

2.2.3. Convergence criterion

In the final stage of each iteration, convergence is checked using both an absolute and a relative termination criterion. The iterative procedure is terminated when both the absolute and the relative adjustments of the equilibrium concentration are smaller than prescribed limits. A typical value for the relative error tolerance is eight significant digits ($\gamma_3 = 10^{-8}$).

2.2.4. Computation of derivatives

The first derivatives of equilibrium concentrations with respect to equilibrium constants and total concentrations are computed directly, in a single step, after the Newton–Raphson method has converged. The solution of the linear system (8) is best accomplished by using the Gaussian elimination (Stoer and Bulirsch, 1991) or a similar matrix decomposition technique. The Gaussian factors obtained in the last iteration of the Newton–Raphson method are then re-used in a single back-substitution step. These tasks are suitably encoded by the routines DGEFA and DGESL from the LINPACK collection of computer programs (Dongarra et al., 1979).

2.2.5. Initial rate equation

The final result of the computation is the initial rate of an enzyme reaction, obtained simply by adding elementary rate terms for the single (possibly reversible) slow step in the reaction mechanism.

For example, if the slow (chemical) step in the reaction mechanism is $E.S \xrightarrow{k_f} E.P$, the overall reaction rate is defined as $v \equiv k_f \times c_{E.S}$, where $c_{E.S}$ is the concentration of E.S at equilibrium. If the slow (chemical) step is reversible, so that the reaction mechanism additionally contains the step $E.S \xleftarrow{k_b} E.P$, the overall reaction rate is defined as $v \equiv k_f \times c_{E.S} - k_b \times c_{E.P}$, where $c_{E.P}$ is the concentration of E.P at equilibrium.

This definition of initial rates is exactly identical to the classical formalism of rapid-equilibrium enzyme kinetics (Segel, 1975). However, an important generalization of the classical treatment is that we do not insist on the enzyme catalyst being present in negligibly small amounts, compared to all ligands (substrates, inhibitors and activators).

2.2.6. Implementation in the software package DYNAFIT

The formalism and algorithms described above were incorporated into a recently updated software package DYNAFIT (Kuzmič, 1996), which is freely available to all academic researchers at http://www.biokin.com/dynafit.

3. Results

A practical application of our generalized rapid-equilibrium enzyme kinetic formalism is illustrated here on a reaction mechanism proposed by Krazeisen et al. (2001) for the inhibition of 17β-hydroxysteroid dehydrogenase type 5 by phytoestrogens. We will first describe how an appropriate mathematical model for the inhibition mechanism can be obtained without any use of algebra. Then, we conduct a heuristic *simulation study*, to design an optimal experiment for discrimination between alternate molecular mechanisms.

Consider the reaction mechanism shown in Scheme 1. The enzyme E first combines with the cofactor C, and subsequently with the steroid substrate S. The inhibitor presumably binds at the cofactor site only. Therefore, in the reaction mechanism we will find both the complex EI (binding of I to the free enzyme), and the complex EIS (binding of steroid substrate to the enzyme–inhibitor complex).

3.1. Mathematical model for the inhibition of 17β-HSD-5

The reaction mechanism in Scheme 1 contains four rapid-equilibrium (reversible) steps, characterized by binary equilibrium constants K_c, K_s, K_i and K_{si}. Each binary equilibrium constant is defined as a *dissociation constant*, e.g., $K_i \equiv c_E \times c_I / c_{EI}$, where c_E, c_I and c_{EI} are concentrations at equi-

			$K_{\rightleftharpoons}$	$k_{\rightarrow}$
$E + C$	$\rightleftharpoons$	EC	K_c	
$EC + S$	$\rightleftharpoons$	ECS	K_s	
ECS	$\rightarrow$	$E + P$		k_{cat}
$E + I$	$\rightleftharpoons$	EI	K_i	
$EI + S$	$\rightleftharpoons$	EIS	K_{si}	

Scheme 1.

librium. In addition, the reaction mechanism contains a single (irreversible) chemical step, characterized by rate constant k_{cat}. Thus, the reaction rate will be calculated as is shown in Eq. (16), where c_{ECS} is the *equilibrium* concentration of the complex ECS.

$$v = k_{cat} \times c_{ECS} \tag{16}$$

The reaction mechanism contains four binary equilibrium steps and eight molecular species that participate in them (note that the product P does *not* participate in rapid-equilibrium steps). Therefore, the stability matrix **B**, defined in Eq. (17), contains four rows and eight columns. Zero elements are represented by period (.) for clarity. The entries in matrix **B** express the total stability constants of molecular complexes in terms of binary dissociation constants. For example, the column labeled ECS gives the total stability constant of complex ECS, $\beta_{ECS} = K_c^{-1}K_s^{-1} = 1/K_cK_s$.

$$\mathbf{B} = \begin{array}{c} \\ K_c \\ K_s \\ K_i \\ K_{si} \end{array} \begin{array}{c} \begin{array}{cccccccc} C & S & E & I & EC & ECS & EI & EIS \end{array} \\ \begin{pmatrix} . & . & . & . & -1 & -1 & . & . \\ . & . & . & . & . & -1 & . & . \\ . & . & . & . & . & . & -1 & -1 \\ . & . & . & . & . & . & . & -1 \end{pmatrix} \end{array} \tag{17}$$

The formula matrix **F** is defined by Eq. (18). Each column describes the composition of a particular molecule in terms of component species. Thus, for example, the rightmost column in the matrix **F**, representing the complex EIS, contains unit entries for the component species E (fourth row), I (fifth row) and S (second row). Note again that the product P does not appear on the list of molecular species, because it does not participate in any rapid-equilibrium steps.

$$\mathbf{F} = \begin{array}{c} \\ C \\ S \\ E \\ I \end{array} \begin{array}{c} \begin{array}{cccccccc} C & S & E & I & EC & ECS & EI & EIS \end{array} \\ \begin{pmatrix} 1 & . & . & . & 1 & 1 & . & . \\ . & 1 & . & . & . & 1 & . & 1 \\ . & . & 1 & . & 1 & 1 & 1 & 1 \\ . & . & . & 1 & . & . & 1 & 1 \end{pmatrix} \end{array} \tag{18}$$

The matrices **B** and **F**, together with the rate Eq. (16), completely represent the mathematical model for the inhibition mechanism in Scheme 1. These matrices, the numerical values of kinetic constants, and the total (analytic) concentrations of species are required for a suitable computer algorithm to calculate the theoretical reaction rate. The matrices **B** and **F** can be either supplied in an explicit form or they can be constructed automatically by a computerized parser, starting from textual data as is shown in Appendix A.2.

To generate automatically the nonlinear algebraic system for equilibrium concentrations of component species, the matrices **B** and **F** are used to form the right-hand sides of Eq. (5), essentially as the mass balance equations for all component species, (19)–(22).

$$f_C: \quad 0 = c_C + \frac{c_E c_C}{K_c} + \frac{c_E c_C c_S}{K_c K_s} - \tilde{c}_C \tag{19}$$

$$f_S: \quad 0 = c_S + \frac{c_E c_C c_S}{K_c K_s} + \frac{c_E c_I c_S}{K_i K_{si}} - \tilde{c}_S \tag{20}$$

$$f_E: \quad 0 = c_E + \frac{c_E c_C}{K_c} + \frac{c_E c_C c_S}{K_c K_s} + \frac{c_E c_I}{K_i} + \frac{c_E c_I c_S}{K_i K_{si}} - \tilde{c}_E \tag{21}$$

$$f_I: \quad 0 = c_I + \frac{c_E c_I}{K_i} + \frac{c_E c_I c_S}{K_i K_{si}} - \tilde{c}_I \tag{22}$$

The Jacobian matrix elements for the example problem, appearing on the left-hand side of Eq. (5), is obtained by differentiating the nonlinear algebraic system (19)–(22) with respect to the state variables (equilibrium concentrations of component species). The resulting matrix elements, automatically generated by the computer, are shown in Eqs. (23)–(38).

$$J_{C,C} = 1 + \frac{c_E}{K_c} + \frac{c_E c_S}{K_c K_s} \tag{23}$$

$$J_{C,S} = \frac{c_E c_C}{K_c K_s} \tag{24}$$

$$J_{C,E} = \frac{c_C}{K_c} + \frac{c_C c_S}{K_c K_s} \tag{25}$$

$$J_{C,I} = 0 \tag{26}$$

$$J_{S,C} = \frac{c_E c_S}{K_c K_s} \tag{27}$$

$$J_{S,S} = 1 + \frac{c_E c_C}{K_c K_s} + \frac{c_E c_I}{K_i K_{si}} \tag{28}$$

$$J_{S,E} = \frac{c_C c_S}{K_c K_s} + \frac{c_I c_S}{K_i K_{si}} \tag{29}$$

$$J_{S,I} = \frac{c_E c_S}{K_i K_{si}} \tag{30}$$

$$J_{E,C} = \frac{c_E}{K_c} + \frac{c_E c_S}{K_c K_s} \tag{31}$$

$$J_{E,S} = \frac{c_E c_C}{K_c K_s} + \frac{c_E c_I}{K_i K_{si}} \tag{32}$$

$$J_{E,E} = 1 + \frac{c_C}{K_c} + \frac{c_C c_S}{K_c K_s} + \frac{c_I}{K_i} + \frac{c_I c_S}{K_i K_{si}} \tag{33}$$

$$J_{E,I} = \frac{c_E}{K_i} + \frac{c_E c_S}{K_i K_{si}} \tag{34}$$

$$J_{I,C} = 0 \tag{35}$$

$$J_{I,S} = \frac{c_E c_I}{K_i K_{si}} \tag{36}$$

$$J_{I,E} = \frac{c_I}{K_i} + \frac{c_I c_S}{K_i K_{si}} \tag{37}$$

$$J_{I,I} = 1 + \frac{c_E}{K_i} + \frac{c_E c_S}{K_i K_{si}} \tag{38}$$

3.2. Convergence of the Newton–Raphson method

The convergence properties of the multidimensional Newton–Raphson method are illustrated in Table 1. In this example, the simulated values of equilibrium constants and rate constants were $K_c = 10$ μM, $K_s = 20$ μM, $K_i = 1$ μM, $K_{si} = 20$ μM and $k_{cat} = 10\,s^{-1}$. The simulated total concentrations were $\tilde{c}_E = 0.01$ μM, $\tilde{c}_S = \tilde{c}_I = 10$ μM and $\tilde{c}_C = 100$ μM.

In the first iteration, the estimated equilibrium concentrations of a component species were set to their analytical concentrations, and the equilibrium concentrations of all molecular

Table 1
Convergence of the Newton–Raphson method in a simulation problem representing the inhibition of 17β-hydroxysteroid dehydrogenase type 5 by phytoestrogens

Equilibrium concentrations	Iteration				
	1	2	3	4	5
c_E (nM)	10	9.996002	0.326171	0.322697	0.322697
c_C (μM)	100	99.99999	99.99513	99.99516	99.99516
c_S (μM)	10	9.999998	9.996796	9.996774	9.996774
c_I (μM)	10	9.999998	9.995195	9.995162	9.995162
c_{EC} (nM)	0.001	99.960014	3.261553	3.226816	3.226816
c_{ECS} (nM)	0.001	49.979997	1.630254	1.612888	1.612888
c_{EI} (nM)	0.001	99.959996	3.260145	3.225412	3.225412
c_{EIS} (nM)	0.001	49.979988	1.629550	1.612186	1.612186

Note that the fifth iteration produced essentially identical equilibrium concentrations, within six significant digits, compared with the previous iteration.

complexes were set to a very small value, using $\gamma_1 = 0.0001$ according to Eq. (14). In four iterations, the equilibrium concentrations of all molecular species converged to within six significant digits. The equilibrium concentration of the reactive complex ECS was $c_{ECS} = 1.612888$ nM, which gives $v = k_{cat} \times c_{ECS} = 16.12888$ nM/s.

3.3. Simulated data

We used the generalized matrix formalism to simulate pseudo-experimental data conforming to the proposed molecular mechanism. According to Krazeisen et al. (2001), 17β-hydroxysteroid reductase type 5 is inhibited by phytosteroids such that the inhibitor binds only to the cofactor site, but not to the steroid substrate site. This is represented by the `[mechanism]` portion of the DYNAFIT script shown in Appendix A.2. The program automatically constructed matrices **B** and **F**, defined for this mechanism in Eqs. (17) and (18), respectively.

The presumed values of kinetic constants were $K_c = 10$ μM, $K_s = 20$ μM, $K_i = 1$ μM, $K_{si} = 20$ μM and $k_{cat} = 10\,s^{-1}$. The inhibitor concentrations were varied between 1 and 16 μM, stepping logarithmically by a factor of 2. Altogether ten rounds of simulations were performed, in which either the steroid substrate or the cofactor was held at a constant concentration, equal to a certain multiple of the corresponding dissociation constant (see the first two columns in Table 2). The concentration of the other substrate was varied.

In particular, the simulated cofactor concentrations were 10, 15, 22.5, 37.75, 50.63, 75.94 and 100 μM. The simulated steroid substrate concentrations were 20, 30, 45, 67.5, 101.25, 151.88 and 200 μM. Each of the ten simulated data sets contained the total of $7 \times 6 = 42$ initial velocity data points, corresponding to seven different substrate concentrations and six inhibitor concentrations. Pseudo-experimental initial velocities were simulated by assuming 1% standard deviation of random noise, relative to the highest velocity in each given data set.

3.4. Model discrimination analysis

Each simulated data set was subjected to least-squares regression analysis, using four candidate mechanistic models. These four mechanistic models are represented by the four different `[mechanism]` portions of the DYNAFIT script shown in Appendix A.3. Note that in contrast to the simulation script in Appendix A.2, the regression script in Appendix A.3 treats the enzyme reaction as if it involved only a single (variable) substrate. This simplification is admissible, because in each series of simulation experiments one of the substrates (either NAD as the cofactor or the steroid substrate) is held at a constant concentration.

The resulting sums of squared deviations, corresponding to each of the four fitting models, were converted to *Akaike weights* (Burnham and Anderson, 2002, p. 75), which serve here as a suitable model discrimination criterion. For example, for the data set shown in Fig. 1, the resulting residual sums of squares are summarized in Table 2. The mixed-type inhibition mechanism produced the lowest sum of squares (RSS = 0.1482), but the most favorable model according to the second-order Akaike information criterion (AICc) is the competitive inhibition model. The reason is that the mixed-type model has a larger number of optimized model parameters (four optimized kinetic constants, $p = 4$) compared to the competitive model ($p = 3$). Consequently, the competitive inhibition model is preferred (AICc = −226.1 indeed is the lowest among all inhibition mechanisms), even though the residual sum of squares is

Table 2
Akaike weights (Burnham and Anderson, 2002, p. 75) from the model discrimination analysis of simulated data shown in Fig. 1

Model	n	p	RSS	AICc	Δ	Akaike weight
Competitive	42	3	0.1551	-226.179	0	0.582
Uncompetitive	42	3	19.0079	-24.217	201.962	0
Noncompetitive	42	3	11.0124	-47.142	179.037	0
Mixed-type	42	4	0.1482	-225.514	0.665	0.418

Explanation of symbols: n, the number of data points; p, the number of adjustable model parameters (kinetic constants) in each model; RSS, the residual sum of squares; AICc, the second-order (i.e., corrected for small data sets) Akaike information criterion (Burnham and Anderson, 2002, p. 66); Δ is the excess AICc for each model, relative to the most favorable model.

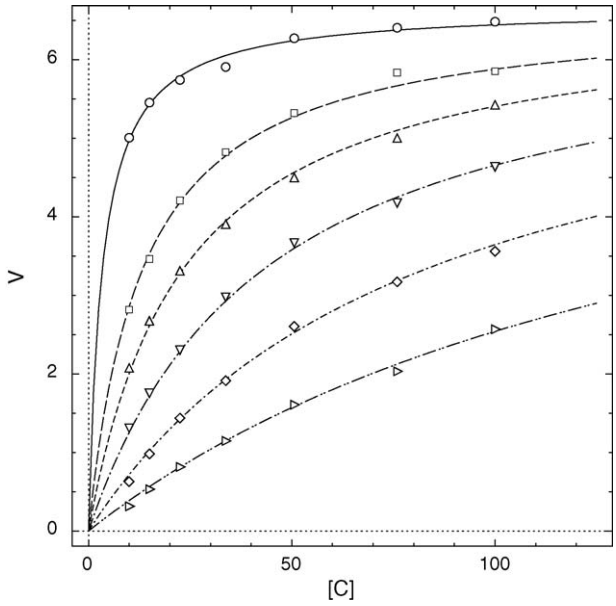

Fig. 1. Inhibition of 17β-hydroxysteroid reductase by phytosteroids, according to the mechanism proposed by Krazeisen et al. (2001). *Symbols*: Artificial data were simulated by using the DYNAFIT script listed in Appendix A.2. The regression analysis, using four alternate kinetic mechanisms, was performed by using the DYNAFIT script listed in Appendix A.3. *Model curves*: Least-squares fit to the *competitive* mechanism.

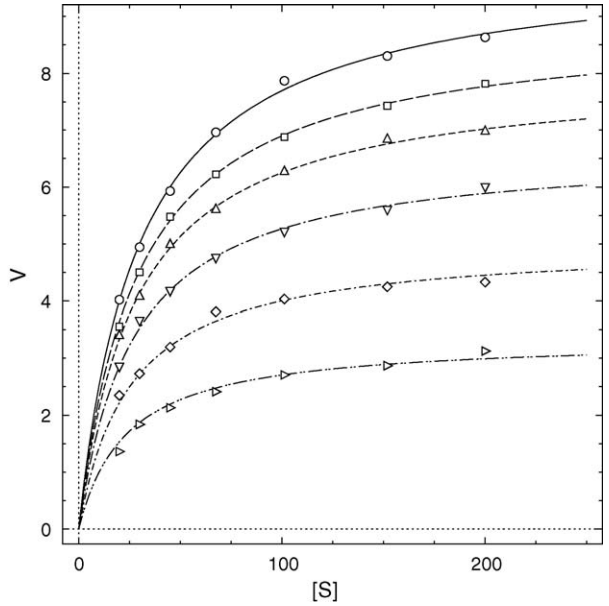

Fig. 2. Inhibition of 17β-hydroxysteroid reductase by phytosteroids, according to the mechanism proposed by Krazeisen et al. (2001). *Symbols*: Artificial data were simulated by using a DYNAFIT script similar to that listed in Appendix A.2, except that the cofactor was held at a constant concentration, and the steroid substrate was varied. The regression analysis, using four alternate kinetic mechanisms, was performed by using a DYNAFIT script similar to that listed in Appendix A.3. *Model curves*: Least-squares fit to the *mixed-type* mechanism.

slightly larger (RSS = 0.1551) than that produced by the mixed-type mechanism.

The competitive inhibition mechanisms was identified as the most plausible kinetic model in all five heuristic simulation experiments, in which the steroid substrate concentration was held constant and the cofactor substrate concentration was varied. This is shown in the first five rows of Table 3.

The results obtained when NAD was the variable substrate, while the steroid concentration was held constant, are illustrated in Figs. 2 and 3 and summarized in the last five rows of Table 3. Here, the competitive inhibition mechanism is never ranked as the most plausible kinetic model. In fact, the most plausible model was either the mixed-type mechanism or the noncompetitive mechanism.

Taken together, these result suggests that the hypothesis (Krazeisen et al., 2001) of phytoestrogens competing for binding to 17β-HSD-5 with the cofactor, but not with the steroid substrate, could be kinetically tested. We also proposed a suitable experimental design (i.e., the choice of substrate and inhibitor concentrations). We showed that the appropriate

Table 3
Summary of Akaike weights (Burnham and Anderson, 2002, p. 75) from the model discrimination analysis of simulated data

Concentration		Mechanism			
Varied	Constant	CMP	UNC	NON	MIX
C	$[S] = 0.25 \times K_s$	0.79	.	.	0.21
C	$[S] = 0.50 \times K_s$	0.70	.	.	0.30
C	$[S] = 1.00 \times K_s$	0.79	.	.	0.21
C	$[S] = 2.00 \times K_s$	0.58	.	.	0.42
C	$[S] = 4.00 \times K_s$	0.77	.	.	0.23
S	$[C] = 0.25 \times K_c$	.	.	.	1.00
S	$[C] = 0.50 \times K_c$	.	.	.	1.00
S	$[C] = 1.00 \times K_c$	.	.	0.01	0.99
S	$[C] = 2.00 \times K_c$	.	.	0.14	0.86
S	$[C] = 4.00 \times K_c$	.	.	0.24	0.76

Mechanisms: CMP, competitive, UNC, uncompetitive, NON, noncompetitive, MIX, mixed-type. Higher Akaike weight (by definition, ranging from zero to one) corresponds to a more plausible model. For further explanation, see text.

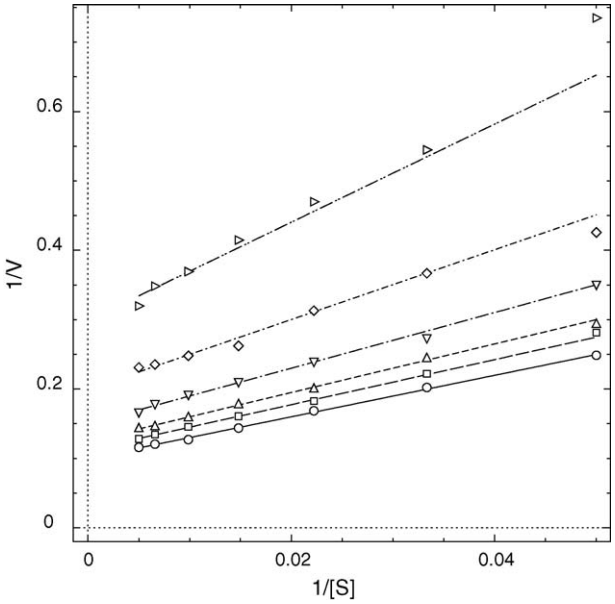

Fig. 3. Lineweaver–Burk plot based on Fig. 2. Note that the best-fit lines do not intersect on the vertical axis.

statistical model discrimination analysis would rely on Akaike weights (Burnham and Anderson, 2002, p. 75).

4. Discussion

In this work, we have described a general numerical method for the analysis of initial-rate enzyme kinetic data, under the rapid-equilibrium approximation. The proposed method does not require any use of algebraic equations. Instead, a matrix formalism based on the *formula matrix* and the *stability matrix* is used to compute the equilibrium composition of molecular complexes. The initial rate in the enzyme reaction is then computed from a single (possibly reversible) nonequilibrium step, based on the mass-action law.

This generalized numerical approach has several advantages. First, a reaction mechanism of arbitrary complexity can be treated, while avoiding often prohibitively complex algebraic rate equations of traditional enzyme kinetics (Segel, 1975). Second, our formalism is applicable without restrictions not only to "classical" (weakly bound) enzyme–inhibitors, but also to "tight-binding" inhibitors, for which the traditional algebraic formalism is not generally applicable. Finally, this numerical formalism is well suited for data fitting by nonlinear least-squares regression, because the derivatives of initial rates with respect to optimized model parameters (i.e., parametric sensitivities) are computed simultaneously with the state variables, resulting in very low computational cost. The method was incorporated into the software package DYNAFIT (Kuzmič, 1996).

As an illustrative example, we have performed a heuristic simulation study of the reaction mechanism proposed by Krazeisen et al. (2001) for the inhibition of 17β-hydroxysteroid dehydrogenase type 5 by phytoestrogens. The salient feature of this proposed mechanism is that the inhibitors (e.g., gibberellin) bind only to the cofactor site on the enzyme, but not to the steroid-binding site. Here, we presented a practical, "workshop-style" description on how this mechanistic hypothesis could be tested by using kinetic methods, without having to deal with complex algebraic equations.

The mechanistic model discrimination analysis could be accomplished by utilizing the DYNAFIT script listed in Appendix A.3. The required experiment involves simultaneously varying the concentrations of the inhibitor and one of the substrates, while holding the concentration of the other substrate at a constant value.

We showed in Table 3 that if the true inhibition mechanism conformed to the proposal by Krazeisen et al. (2001), and if the cofactor (NAD) were varied simultaneously with the inhibitor, a model discrimination analysis utilizing the second-order Akaike Information Criterion would indeed favor the competitive mechanism. Ranked as a close second, according to AICc values, is the mixed-type mechanism. However, upon closer examination of the kinetic constants obtained in the regression analysis, it is seen that the noncompetitive component of inhibitor binding would be negligibly weak, compared to the principal binding mode (competitive with NAD).

For example, in the case of the data set shown in Fig. 1, the best-fit values of inhibition constants appearing in the mixed-type mechanism were $K_i = 0.357 \pm 0.019$ μM and $K_{is} = 232.2 \pm 175.3$ μM. Note that the inhibition constant K_{is} is approximately 650 times larger than K_i. Also, K_{is} it is affected by a very large uncertainty, as measured by the formal standard error. In fact, the upper end of the 99% confidence interval could not be determined, which means that at the 99% confidence level the constant K_{is} plausibly could be infinitely large.

Table 4
"True" (simulated) values of kinetic constants, according to the reaction mechanism in Scheme 1 (see also DYNAFIT script in Appendix A.2), and the corresponding best-fit values to the *mixed-type inhibition* model (see the last portion of the DYNAFIT script in Appendix A.3)

$\tilde{c}_C/K_c$	K_m	k_{cat}	K_i	K_{is}
0.25	102.3	10.1	1.33	0.25
0.5	62.8	10.1	1.82	0.48
1	41.1	10.1	1.90	1.03
2	29.9	10.0	2.93	2.01
4	24.6	9.9	5.86	3.95
"True" value	20	10	1	20

The concentration of the steroid substrate was varied as is described in the text. The concentration of the cofactor was held constant as is shown in the first column.

In contrast, if the steroid substrate were varied simultaneously with the inhibitor, a model discrimination analysis utilizing the second-order Akaike information criterion would favor the mixed-type (not competitive) mechanism. This is shown in the last five rows of Table 3. In this context, it is interesting to examine the best-fit values of the inhibition constants and compare them with the "true" (i.e., simulated) values. The relationship between the "true" and fitted values is shown in Table 4.

An important aspect of the results in Table 4 is that the best-fit value of the inhibition constant K_{is} is vastly different from its "true" or simulated value. If the concentration of the steroid substrate were varied at a very low cofactor concentration (relative to the Michaelis constant for NAD), the best-fit value of K_{is} would also appear very low. This result points to the high importance of proper choice of concentrations in any actual experimental study. In particular, if the steroid substrate were considered as the variable component, the cofactor concentration should be as close to saturation as is practically feasible.

In summary, we have demonstrated in a heuristic simulation study that by utilizing a properly chosen experimental design, it is possible to use kinetic methods to gain evidence in favor (or against) the structural hypothesis proposed by Krazeisen et al. (2001) for the inhibition of 17β-hydroxysteroid dehydrogenase type 5 by phytoestrogens. If inhibitors such as gibberellin were in fact binding only at the cofactor site, it is expected that the kinetic pattern observed at constant NAD concentration and varied steroid concentration would appear to be *mixed-type*, but only if the NAD concentration were kept sufficiently high. In contrast, if the steroid concentration were held constant (at any value, relative to the corresponding Michaelis constant), the kinetic pattern would correspond to *competitive* inhibition.

It is also clear from our results that the apparent inhibition constants determined under experimental conditions simulated

here, under which one of the substrates is held constant (as is commonly done in model discrimination studies), the best-fit values of inhibition constants would bear very little resemblance to the true values of inhibition constants. In fact, the true values of K_i and K_{is} could be determined only if at least three reaction components (both substrates and the inhibitor in question) were varied simultaneously.

Probably the most important result is that practically oriented enzymologists, who wish to employ thorough kinetic investigations but lack the expertise in mathematics, can now use an updated version of the software DYNAFIT (Kuzmič, 1996), which implements the matrix method for generalized rapid-equilibrium enzyme kinetics described in this paper. The DYNAFIT software package is available for download free of charge to all academic researchers at http://www.biokin.com/dynafit.

Acknowledgments

I thank Dr. Jerzy Adamski (GSF National Research Center for Health and Environment), and other organizers of the May 2005 Workshop on 11β- and 17β-Hydroxysteroid Dehydrogenases (Schloß Elmau, Germany), for the invitation to present this work at the workshop.

Appendix A

A.1. Derivation of the mathematical model

This Appendix shows the derivation of matrix and vector elements that are required in the multidimensional Newton–Raphson method, and in the computation of first derivatives of equilibrium concentrations with respect to model parameters (reaction equilibrium constants and total or analytic concentrations).

Elements of the Jacobian matrix are obtained by differentiation of mass balance equations (A.1) as is shown in Eq. (A.2).

$$f_i = \sum_{j=1}^{n_S} F_{i,j} c_j - \sum_{j=1}^{n_S} F_{i,j} \tilde{c}_j; \quad i = 1, 2, \ldots, n_E \tag{A.1}$$

$$\begin{aligned} J_{i,j} \equiv \frac{\partial f_i}{\partial c_j} &= \frac{\partial}{\partial c_j} \left\{ \sum_{k=1}^{n_S} F_{i,k} \beta_k \prod_{l=1}^{n_E} c_l^{F_{l,k}} - \sum_{k=1}^{n_S} F_{i,k} \tilde{c}_k \right\} \\ &= \sum_{k=1}^{n_S} F_{i,k} F_{j,k} c_j^{F_{j,k}-1} \beta_k \prod_{\substack{l=1 \\ l \neq j}}^{n_E} c_l^{F_{l,k}} \\ &= \sum_{k=1}^{n_S} F_{i,k} F_{j,k} c_j^{-1} \beta_k \prod_{l=1}^{n_E} c_l^{F_{l,k}} \\ &= \sum_{k=1}^{n_S} F_{j,k} F_{i,k} \frac{c_k}{c_j}; \quad i, j = 1, \cdots, n_E \end{aligned} \tag{A.2}$$

The deviations from mass balance **f** depend on equilibrium concentrations **c** and on parameters **p**. In their turn the equilibrium concentrations depend on the parameters **p** also. In particular, we seek the vector $\partial \mathbf{c}/\partial p$ of partial derivatives with respect to the given parameter p. At equilibrium the deviations **f** vanish, $\mathbf{f}(\mathbf{c}, \mathbf{p}) = 0$. Both sides of this equation can be differentiated by using the chain rule of calculus (Kreyszig, 1993, p. 472). Thus the derivatives $\partial \mathbf{c}/\partial p$ are obtained by solving the linear system (A.4). Note that the matrix **J** also appears in Eq. (5). Therefore, the Gaussian factors from the final matrix decomposition within the iterative Newton–Raphson method can be re-used in a single additional back-substitution.

$$\begin{aligned} \frac{\partial \mathbf{f}(\mathbf{c}, \mathbf{p})}{\partial p} &= \frac{\partial \mathbf{f}(\mathbf{c}, \mathbf{p})}{\partial \mathbf{c}} \cdot \frac{\partial \mathbf{c}}{\partial p} + \frac{\partial \mathbf{f}(\mathbf{c}, \mathbf{p})}{\partial \mathbf{p}} \cdot \frac{\partial \mathbf{p}}{\partial p} \\ &= \frac{\partial \mathbf{f}(\mathbf{c}, \mathbf{p})}{\partial \mathbf{c}} \cdot \frac{\partial \mathbf{c}}{\partial p} + \frac{\partial \mathbf{f}(\mathbf{c}, \mathbf{p})}{\partial p} = 0 \end{aligned} \tag{A.3}$$

$$\mathbf{J} \cdot \frac{\partial \mathbf{c}}{\partial p} = -\frac{\partial \mathbf{f}}{\partial p} \tag{A.4}$$

The form of right-hand side vector above depends on whether the parameter p is an equilibrium constant or an analytic concentration. If p is a reaction equilibrium constant K_u, than we differentiate function **f** as is shown in Eq. (A.5). Derivatives of component concentrations with respect to the given analytic concentration c_u are obtained as is shown in Eq. (A.6).

$$\begin{aligned} \frac{\partial f_i}{\partial K_u} &= \frac{\partial}{\partial K_u} \left\{ \sum_{j=1}^{n_S} F_{i,j} \prod_{k=1}^{n_R} K_k^{B_{k,j}} \prod_{k=1}^{n_E} c_k^{F_{k,j}} - \sum_{j=1}^{n_S} F_{i,j} \tilde{c}_j \right\} \\ &= \sum_{j=1}^{n_S} F_{i,j} B_{u,j} K_u^{B_{u,j}-1} \prod_{\substack{k=1 \\ k \neq u}}^{n_R} K_k^{B_{k,j}} \prod_{k=1}^{n_E} c_k^{F_{k,j}} \\ &= \sum_{j=1}^{n_S} F_{i,j} B_{u,j} K_u^{-1} \prod_{k=1}^{n_R} K_k^{B_{k,j}} \prod_{k=1}^{n_E} c_k^{F_{k,j}} \\ &= \sum_{j=1}^{n_S} F_{i,j} B_{u,j} K_u^{-1} \beta_j \prod_{k=1}^{n_E} c_k^{F_{k,j}} \\ &= K_u^{-1} \sum_{j=1}^{n_S} B_{u,j} F_{i,j} c_j; \quad i = 1, \cdots, n_E \end{aligned} \tag{A.5}$$

$$\begin{aligned} \frac{\partial f_i}{\partial \tilde{c}_u} &= \frac{\partial}{\partial \tilde{c}_u} \left\{ \sum_{j=1}^{n_S} F_{i,j} \prod_{k=1}^{n_R} K_k^{B_{k,j}} \prod_{k=1}^{n_E} c_k^{F_{k,j}} - \sum_{j=1}^{n_S} F_{i,j} \tilde{c}_j \right\} \\ &= -\sum_{j=1}^{n_S} F_{i,j} \delta_{u,j}; \quad i = 1, \cdots, n_E \end{aligned} \tag{A.6}$$

The derivatives of complex species are derived by differentiation of both sides in Eq. (1). If the parameter p is an equilibrium constant, we obtain formula (A.7). If the parameter p is an analytic concentration, we obtain formula (A.8) in a

similar fashion.

$$\begin{aligned}\frac{\partial c_j}{\partial K_u} &= \frac{\partial}{\partial K_u}\left\{\prod_{i=1}^{n_\mathrm{R}} K_i^{B_{i,j}} \prod_{i=1}^{n_\mathrm{E}} c_i^{F_{i,j}}\right\} \\ &= B_{u,j} K_u^{B_{u,j}-1} \prod_{\substack{i=1 \\ i\neq u}}^{n_\mathrm{R}} K_k^{B_{i,j}} \prod_{i=1}^{n_\mathrm{E}} c_k^{F_{i,j}} \\ &\quad + \prod_{i=1}^{n_\mathrm{R}} K_i^{B_{i,j}} \sum_{i=1}^{n_\mathrm{E}} F_{i,j} c_i^{F_{i,j}-1} \prod_{\substack{k=1 \\ k\neq i}}^{n_\mathrm{E}} c_k^{F_{k,j}} \frac{\partial c_i}{\partial K_u} \\ &= B_{u,j} K_u^{-1} \beta_j \prod_{i=1}^{n_\mathrm{E}} c_k^{F_{i,j}} + \sum_{i=1}^{n_\mathrm{E}} F_{i,j} c_i^{-1} \frac{\partial c_i}{\partial K_u} \beta_j \prod_{k=1}^{n_\mathrm{E}} c_k^{F_{k,j}} \\ &= B_{u,j} K_u^{-1} \beta_j \prod_{i=1}^{n_\mathrm{E}} c_k^{F_{i,j}} + \sum_{i=1}^{n_\mathrm{E}} F_{i,j} c_i^{-1} \frac{\partial c_i}{\partial K_u} \beta_j \prod_{k=1}^{n_\mathrm{E}} c_k^{F_{k,j}} \\ &= c_j \left\{ B_{u,j} K_u^{-1} + \sum_{i=1}^{n_\mathrm{E}} F_{i,j} c_i^{-1} \frac{\partial c_i}{\partial K_u} \right\}; \\ j &= n_\mathrm{E}+1, \cdots, n_\mathrm{S}\end{aligned} \tag{A.7}$$

$$\begin{aligned}\frac{\partial c_j}{\partial \tilde{c}_u} &= \frac{\partial}{\partial \tilde{c}_u}\left\{\beta_j \prod_{i=1}^{n_\mathrm{E}} c_i^{F_{i,j}}\right\} = \beta_j \sum_{i=1}^{n_\mathrm{E}} F_{i,j} c_i^{F_{i,j}-1} \prod_{\substack{k=1 \\ k\neq i}}^{n_\mathrm{E}} c_k^{F_{k,j}} \frac{\partial c_i}{\partial \tilde{c}_u} \\ &= \beta_j \sum_{i=1}^{n_\mathrm{E}} F_{i,j} c_i^{-1} \prod_{k=1}^{n_\mathrm{E}} c_k^{F_{k,j}} \frac{\partial c_i}{\partial \tilde{c}_u} = c_j \left\{ \sum_{i=1}^{n_\mathrm{E}} F_{i,j} c_i^{-1} \frac{\partial c_i}{\partial \tilde{c}_u} \right\}; \\ j &= n_\mathrm{E}+1, \cdots, n_\mathrm{S}\end{aligned} \tag{A.8}$$

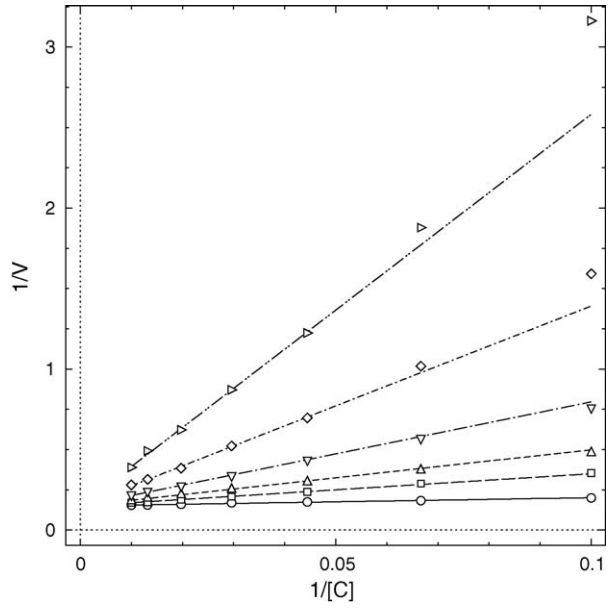

Fig. A.1. Lineweaver–Burk plot based on Fig. 1. Note that the best-fit lines do intersect on the vertical axis.

All of the above formulas are derived automatically, and transparently to the user, by the software package DYNAFIT (Kuzmič, 1996).

A.2. DYNAFIT input file for simulation

This Appendix lists an input file for the software package DYNAFIT, which was used to generate the simulated data shown in Figs. 1 and A.1.

```
;-----------------------------------------------------
[task]
   task = simulate
   data = velocities
[mechanism]
   E + NAD <===> E.NAD          :    Km(NAD)    dissoc.
   E.NAD + S <===> E.NAD.S      :    Km(S)      dissoc.
   E.NAD.S ---> E + NADH + P    :    kcat
   E + I <===> E.I              :    Ki         dissoc.
   E.I + S <===> E.I.S          :    Kis        dissoc.
[constants] ; all micromolar
   Km(NAD) = 10
   Km(S)   = 20
   kcat    = 10
   Ki      = 1
   Kis     = 20
[concentrations] ; all micromolar
   E = 0.001
   S = 40         ; [S] = 2 Km(S)
[responses]
   P = 1000
[progress]
   rapid equilibrium
[velocities]
   directory ./demo/17b-HSD5/data/S=2.00xKm
   extension txt
   mesh      logarithmic from 10 to 100 step 1.5
   error     percent 1
   variable  NAD
   plot      Lineweaver-Burk
   file      i0  |  concentration I = 0
   file      i1  |  concentration I = 1
   file      i2  |  concentration I = 2
   file      i4  |  concentration I = 4
   file      i8  |  concentration I = 8
   file      i16 |  concentration I = 16
[output]
   directory ./demo/17b-HSD5/output/S_2.00xKm-simulate
[end]
```

A.3. DYNAFIT input file for model discrimination

This Appendix lists an input file for the software package DYNAFIT, which was used for the model discrimination analysis illustrated in Figs. 1 and A.1.

```
;------------------------------------------------
[task]
   task = fit
   data = velocities
   model = competitive ?
[mechanism]
   E + Sub <===> E.Sub        :   Km      dissoc.
   E.Sub ---> E + P           :   kcat
   E + I <===> E.I            :   Ki      dissoc.
[constants] ; all micromolar
   Km      = 10 ?
   kcat    =  5 ?
   Ki      =  1 ?
[concentrations] ; all micromolar
   E = 0.001
[responses]
   P = 1000
[progress]
   rapid equilibrium
[velocities]
   directory ./demo/17b-HSD5/data/S=2.00xKm
   extension txt
   variable  Sub
   plot      Lineweaver-Burk
   file      i0  |  concentration I = 0
   file      i1  |  concentration I = 1
   file      i2  |  concentration I = 2
   file      i4  |  concentration I = 4
   file      i8  |  concentration I = 8
   file      i16 |  concentration I = 16
[output]
   directory ./demo/17b-HSD5/output/S_2.00xKm-fit
[settings]
   <Marquardt>
      Interrupt = 200
;------------------------------------------------
[task]
   task = fit
   data = velocities
   model = uncompetitive ?
[mechanism]
   E + Sub <===> E.Sub        :   Km      dissoc.
   E.Sub ---> E + P           :   kcat
   E.Sub + I <===> E.Sub.I    :   Ki      dissoc.
;------------------------------------------------
[task]
   task = fit
   data = velocities
   model = noncompetitive ?
[mechanism]
   E + Sub <===> E.Sub        :   Km      dissoc.
   E.Sub ---> E + P           :   kcat
   E + I <===> E.I            :   Ki      dissoc.
   E.Sub + I <===> E.Sub.I    :   Ki      dissoc.
;------------------------------------------------
[task]
   task = fit
   data = velocities
   model = mixed ?
[mechanism]
   E + Sub <===> E.Sub        :   Km      dissoc.
   E.Sub ---> E + P           :   kcat
   E + I <===> E.I            :   Ki      dissoc.
   E.Sub + I <===> E.Sub.I    :   Kis     dissoc.
[constants]
   Km      = 10 ?
   kcat    =  5 ?
   Ki      =  1 ?
   Kis     =  1 ?
[end]
```

References

Beck, M.T., Nagypál, I., 1990. Chemistry of Complex Equilibria. Ellis Horwood, Chichester.

Burnham, K.B., Anderson, D.R., 2002. Model Selection and Multimodel Inference: A Practical Information-Theoretic Approach, second ed. Springer–Verlag, New York.

Dongarra, J.J., Bunch, J.R., Moler, C.B., Stewart, G.W., 1979. LINPACK User's Guide. Society for Industrial and Applied Mathematics, Philadelphia.

Krazeisen, A., Breitling, R., Moeller, G., Adamski, J., 2001. Phytoestrogens inhibit human 17β-hydroxysteroid dehydrogenase type 5. Mol. Cell. Endocrinol. 171, 151–162.

Kreyszig, E., 1993. Advanced Engineering Mathematics, seventh ed. John Wiley, New York.

Kuzmič, P., 1996. Program DYNAFIT for the analysis of enzyme kinetic data: Application to HIV proteinase. Anal. Biochem. 237, 260–273.

Kuzmič, P., 1998. Fixed-point methods for computing the equilibrium composition of complex biochemical mixtures. Biochem. J. 331, 571–575.

Kuzmič, P., Ng, K.Y., Heath, T.D., 1992. Mixtures of tight-binding enzyme–inhibitors: kinetic-analysis by a recursive rate-equation. Anal. Biochem. 200, 68–73.

Press, W.H., Teukolsky, S.A., Vetterling, W.T., Flannery, B.P., 1992. Numerical Recipes in C. Cambridge University Press, Cambridge.

Segel, I.H., 1975. Enzyme Kinetics. Wiley, New York.

Smith, W.R., Missen, R.W., 1982. Chemical Reaction Equilibrium Analysis: Theory and Algorithms. Wiley-Interscience, New York.

Stoer, J., Bulirsch, R., 1991. Introduction to Numerical Analysis. Springer–Verlag, New York.

Williams, J.W., Morrison, J.F., 1979. The kinetics of reversible tight-binding inhibition. Meth. Enzymol. 63, 437–467.